Site symmetry and deformation-potential constants of Al-X acceptors in silicon

H. R. Chandrasekhar
Department of Physics, University of Missouri—Columbia, Columbia, Missouri 65211

A. K. Ramdas
Department of Physics, Purdue University, West Lafayette, Indiana 47907

(Received 29 July 1985)

A quantitative piezospectroscopic study of the acceptor spectrum of X centers of aluminum in silicon shows that, in contrast to the group-III acceptors in silicon, they have a trigonal rather than the tetrahedral symmetry with preferred axes along the ⟨111⟩ direction. Uniaxial stress along the ⟨111⟩ and ⟨110⟩ directions separates these centers into two inequivalent sets with 1:3 and 1:1 ratios, respectively. However, the ⟨100⟩ stress leaves them unaffected. Deformation-potential constants associated with the lifting of orientational degeneracy and those corresponding to the excited states of the impurity are determined.

I. INTRODUCTION

During the investigation of the excitation spectra[1] of group-III acceptors in silicon, Onton *et al.*[2] observed an additional set of lines in aluminum-doped, crucible-grown silicon; these lines, designated $X1$—$X4$, appeared to be related to the aluminum impurities and were ascribed to aluminum-oxygen centers. Similar X centers have since been discovered in indium-doped silicon.[3,4] It appears that the presence of the X centers degrades the performance of the extrinsic infrared detectors which exploit the photoionization of the substitutional Al or In acceptors. Several models for the X centers have been proposed in the literature. Some involve nearest-neighbor[5] or distant[6] pairs of the dominant acceptor with another impurity, whereas an interstitial or vacancy-related defect[7] has been suggested on the basis of radiation-damage studies. Electron-paramagnetic-resonance studies[8] indicated that In-X centers are due to In-Fe pairs.[9] In the present paper we report the results of a detailed piezospectroscopic study of the excitation lines of Al-X centers. The polarization of the stress-induced components, depopulation effects, and the behavior with compressive force in different crystallographic directions—all studied with a quantitative stress cell—have enabled us to deduce the site symmetry of the Al-X centers and the deformation-potential constants characterizing the orientational degeneracy of its ground state. Our results are consistent with those of Jones *et al.*,[5] who employed, however, only a fixed, unknown stress.

II. EXPERIMENTAL

A Perkin-Elmer E-1 monochromator and a zinc-doped germanium photoconductive detector were used in the present investigation.[10] A Perkin-Elmer wire-grid polarizer with a AgBr substrate was used to polarize the electric vector **E** of the infrared radiation either parallel or perpendicular to the applied compressive force **F**. A low-temperature quantitative stress cryostat[11] with a modified sample-mounting procedure yielded uniform stress up to 2.5 kbar. The measurements reported in this paper were performed with liquid helium as a coolant. The samples were obtained from crucible-grown, aluminum-doped sil-

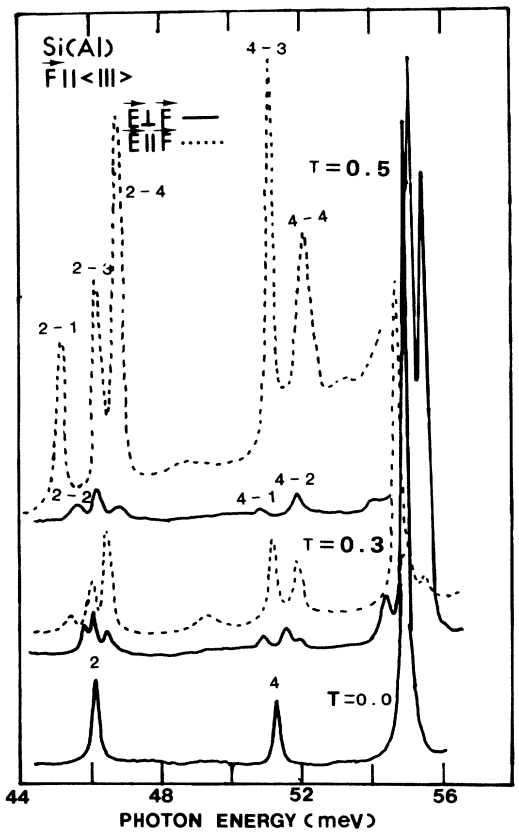

FIG. 1. Effect of a ⟨111⟩ compression on lines 2 and 4 of the Al-X center acceptor spectrum in silicon for the hole concentration $p(300\ \mathrm{K})=1.6\times10^{16}\ \mathrm{cm}^{-3}$. The solid curves are for the electric vector **E**⊥**F**, the applied force, and the dashed curves are for **E**||**F**. Also shown in the spectrum is line 1 of the aluminum acceptor. The curves are for different compressive stresses T (kbar).

TABLE I. Experimental zero-stress positions (in meV) of the Al-X excitation lines in silicon. p is the concentration of holes.

Line no.	Present data	Onton *et al.*[a]	Scott[b]
1	41.95		41.91
2	46.14	46.12	46.12
3	49.98		50.09
4	51.29	51.26	51.33

[a]Reference 2; $p=1.6\times10^{16}$ cm^{-3}.
[b]Reference 4; $p=8\times10^{16}$ cm^{-3}.

icon ingots; they exhibited the characteristic 9μm oxygen vibrational band as well as the excitation spectrum associated with residual boron acceptors.[1]

III. EXPERIMENTAL RESULTS

The excitation lines 2 and 4 of Si(Al-X) and line 1 of Si(Al) are shown in Fig. 1, the identification being based on the comparison of the binding energies of the final states as explained in Ref. 1. The line positions are listed in Table I and compared with the other measurements reported in the literature. The intensities of lines 2 and 4 allow a detailed analysis of their stress-induced components.

Figures 1–3 show the effect of uniaxial stress on lines 2 and 4 of the X-center spectrum of aluminum for applied compressive force **F** along ⟨111⟩, ⟨100⟩, and ⟨110⟩, respectively. The electric vector **E** of the radiation was either parallel or perpendicular to **F**. Figures 4–6 show the energies of the stress-induced components for **F** along ⟨111⟩, ⟨100⟩, and ⟨110⟩, respectively. It can be seen

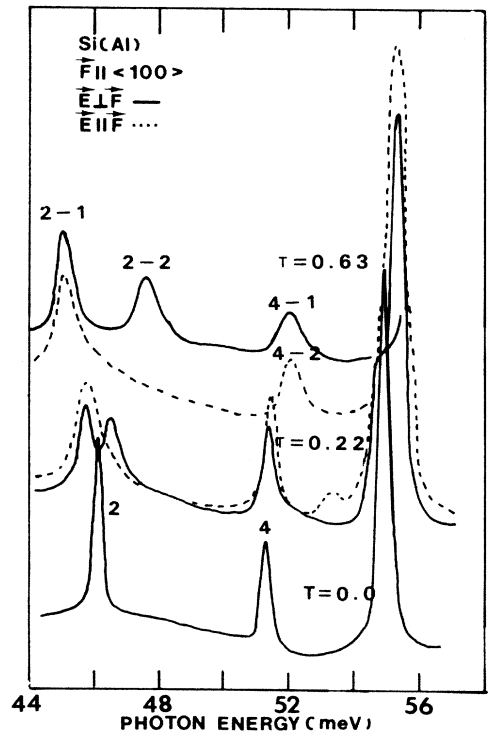

FIG. 2. Effect of a ⟨100⟩ compression T (kbar) on lines 2 and 4 of the Al-X center spectrum. $p(300\text{ K})=1.6\times10^{16}$ cm^{-3}. Line 1 of the aluminum acceptor is also shown.

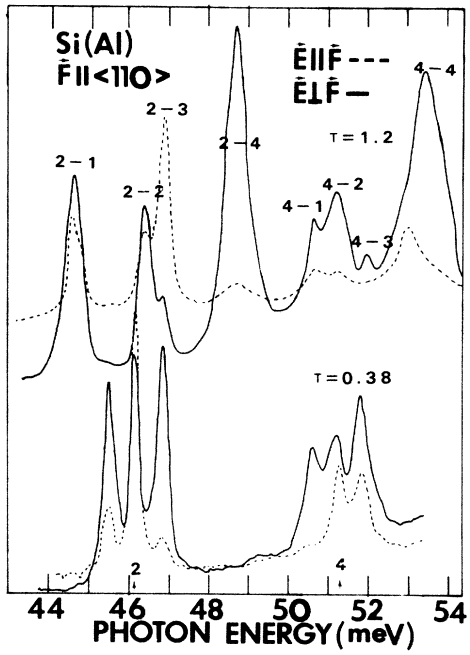

FIG. 3. Effect of a ⟨110⟩ compression T (kbar) on lines 2 and 4 of the Al-X center spectrum. $p(300\text{ K})=1.6\times10^{16}$ cm^{-3}. The vertical arrows at the bottom of the figure indicate the zero-stress positions of lines 2 and 4.

from Figs. 1 and 4 that lines 2 and 4 split into four components for **F**||⟨111⟩ up to the maximum stress employed in our studies. Also shown for comparison in Fig. 1 is line 1 of the aluminum acceptor and its splitting under an uniaxial stress of 0.3 kbar. Line 1 splits into four components also. However, there are important differences in the behavior of the stress-induced components of the aluminum acceptor and those of the Al-X center. We return to this later. For **F**||⟨100⟩, line 2 of the Al-X center

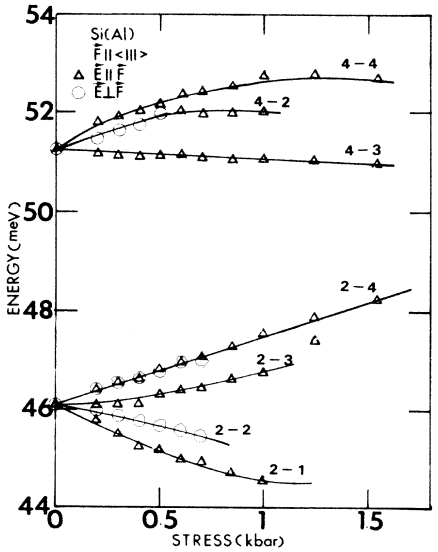

FIG. 4. Stress dependence of the energies of the stress-induced components of lines 2 and 4 of Al-X centers in silicon for **F**||⟨111⟩. The triangles and circles are for the electric vector **E** parallel and perpendicular to **F**, respectively. The components are labeled as described in the text.

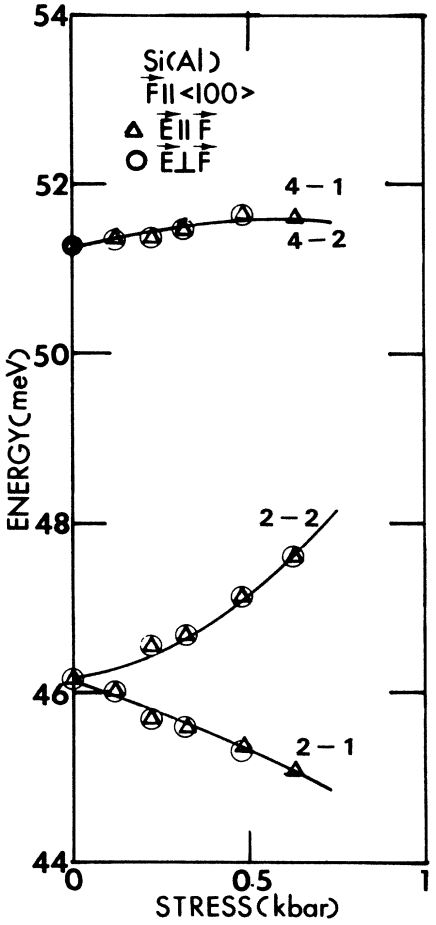

FIG. 5. Same as Fig. 4 for F||⟨100⟩.

splits into two components, whereas line 4 does not (Figs. 2 and 4). Line 1 of the Al acceptor shown in this figure also essentially shows one component close to the zero-stress position. For F||⟨110⟩, line 2 splits into three components at moderate stresses. At higher stresses, however, the middle component splits further, leading to four stress-induced components. Line 4 also splits into four components, though at high stresses more lines appear due to some components from the weak line 3 and higher states of the X center being resolved from the main line-4 component. (See Figs. 3 and 6.)

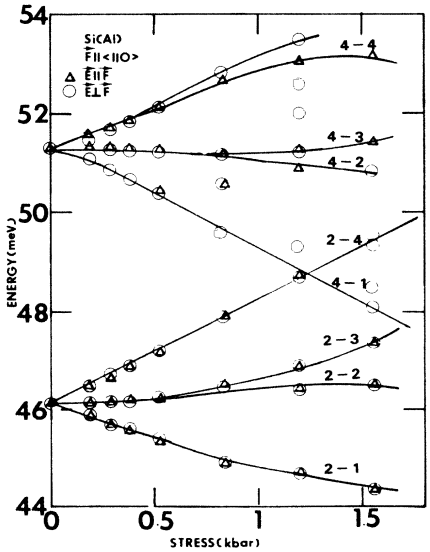

FIG. 6. Same as Fig. 4 for F||⟨110⟩.

The low-energy components of the aluminum acceptor decrease in intensity with increased stress and vanish at higher stresses. This is interpreted[1,2] as due to the stress-induced splitting of the fourfold Γ_8 ground state (site symmetry T_d) into twofold states. The population of the upper ground state depletes as it moves up with increased stress according to the Boltzmann factor. The components originating from the upper ground state consequently decrease in intensity. We shall refer to this effect as the "depopulation effect." The depopulation effect is the fingerprint of a split ground state. Lines 1—4 of group-III acceptors exhibit this effect, leading to the assignment of a Γ_8 ground state for all these acceptors.[2,12,13] Surprisingly, the low-energy components of lines 2 and 4 of Al-X centers do not exhibit the depopulation effect. This is true for all three principal stress directions. This suggests that the ground state of the Al-X center has a lower symmetry than Γ_8, and hence would not be further split into two components under uniaxial stress.

If the excited state associated with line 2 of the Al-X center has a fourfold Γ_8 symmetry like all group-III acceptors, it should split into two levels under uniaxial stress. Hence, one would observe two stress-induced components due to transitions from the ground state which does not split under stress. This is in contrast to the four components observed in group-III acceptors due to the splitting of both the fourfold ground and excited states into Kramers doublets. Figures 1—6 reveal that line 2 of the Al-X center splits into four components for F||⟨111⟩ and ⟨110⟩, and two components for F||⟨100⟩. Jones *et al.*[5] postulated the site symmetry of the impurity to be trigonal instead of tetrahedral and oriented along the ⟨111⟩ direction. If this were the case, for F||⟨111⟩, the impurity centers along [111] would be affected differently than those along [1 $\bar{1}$ $\bar{1}$], [$\bar{1}$ $\bar{1}$ 1], and [$\bar{1}$ 1 $\bar{1}$]. This would lead to two sets of energy levels, with one set displaced three times below the center of gravity of the other displaced above it. (If the sign of the shear deformation potential is positive the situation is reversed.) For F||[110] the impurity centers along [111] and [$\bar{1}$ $\bar{1}$ 1] would be affected differently than those along [1 $\bar{1}$ $\bar{1}$] and [$\bar{1}$ 1 $\bar{1}$]. This leads to two levels equally displaced from the center of gravity. For F||[100], all four sets of centers are affected equally and remain degenerate under stress. The experimental results are consistent with this postulate, leading us to believe that the Al-X centers depart slightly from the usual tetrahedral symmetry of a substitutional group-III acceptor and have a ⟨111⟩-oriented trigonal symmetry.[14]

IV. DISCUSSION

On the basis of the experimental evidence presented in the preceding section, we assume there are four types of Al-X centers directed along [111], [1 $\bar{1}$ $\bar{1}$], [$\bar{1}$ $\bar{1}$ 1], and [$\bar{1}$ 1 $\bar{1}$] and label them 1, 2, 3, and 4, respectively. For an arbitrary direction of external applied force, the energy

shifts $\delta E^{(j)}$ of all four $\langle 111 \rangle$ centers would be different. This yields four sublevels for each of the excited states due to the breaking of orientational degeneracy alone. We use arguments similar to Herring's deformation-potential analysis[15] in the following. The following features for the stress along high-symmetry directions should be noted. For $\mathbf{F}||[111]$, $\delta E^{(1)}=-3\delta E^{(2),(3),(4)}$. This leads to two sublevels with one of them displaced three times further above or below the center of gravity than the other displaced in the opposite direction. The signs of the shear-deformation-potential constant χ associated with this shift and the stress T (negative for compression) determine whether a level moves up or down in energy. We define the splitting to be linear in stress and given by

$$\delta E^{(1)}-\delta E^{(2),(3),(4)}=\tfrac{2}{3}\chi_{\langle 111\rangle}Ts_{44} . \quad (1)$$

Here, s_{ij} are elastic compliance coefficients. For $\mathbf{F}||[100]$, $\delta E^{(j)}=0$ for all j. The orientational degeneracy is not lifted. For $\mathbf{F}||[110]$, $\delta E^{(1),(3)}=-\delta E^{(2),(4)}$. This leads to sublevels equally displaced from the center of gravity. The splitting is linear with stress given by

$$\delta E^{(1),(3)}-\delta E^{(2),(4)}=\tfrac{1}{3}\chi_{\langle 110\rangle}TS_{44} . \quad (2)$$

Due to the reduction in site symmetry of the impurity under uniaxial stress, there are additional splittings of the lines which have been studied both theoretically[13,16] and experimentally.[12,17] A substitutional group-III acceptor in silicon or germanium is characterized by a set of fourfold energy states separated by twofold partners by the spin-orbit interaction. For group-III acceptors in silicon, the ground state and the first three excited states have a fourfold Γ_8 symmetry.[1,2] Under uniaxial stress, in general, the Γ_8 state splits into two twofold states. For silicon, due to the small spin-orbit splitting the stress-induced mixing between the spin-orbit-split states should be taken into account. This effect leads to the nonlinear stress dependence of the stress-induced component. Following Ref. 13, for $\mathbf{F}$ along $\langle 111 \rangle$, the eigenvalues of the stress-induced components of a Γ_8 state are

$$a(S_{11}+2S_{12})T+\frac{\Delta_{111}}{2}$$

and

$$a(S_{11}+2S_{12})T-\frac{\Delta_{111}}{2}\left[1+\frac{\Delta_{111}}{\lambda}\right] .$$

For $\mathbf{F}$ along $\langle 100 \rangle$, the corresponding eigenvalues are

$$a(S_{11}+2S_{12})T+\frac{\Delta_{100}}{2}$$

and

$$a(S_{11}+2S_{12})T-\frac{\Delta_{100}}{2}\left[1+\frac{\Delta_{100}}{\lambda}\right] .$$

We have used the usual definitions $\Delta_{111}=(d/\sqrt{3})S_{44}T$ and $\Delta_{100}=2b(S_{11}-S_{12})T$. Here, a, b, and d are the deformation-potential constants associated with the given impurity state. λ is the spin-orbit splitting of the respective impurity state. For $\mathbf{F}||\langle 110 \rangle$, the stress-induced splitting of the fourfold Γ_8 state, Δ_{110}, is $(\frac{1}{3}\mu)^{1/2}(1+\nu/\mu\lambda)$. This reduces to the familiar expression $4\Delta_{110}^2=3\Delta_{111}^2+\Delta_{100}^2$ for $\nu/\mu \ll \lambda$. Here, ν and μ are defined as $\mu=\frac{3}{4}(\Delta_{100}^2+3\Delta_{111}^2)$ and $\nu=\frac{3}{16}\Delta_{100}(9\Delta_{111}^2-\Delta_{100}^2)$. These results together with the splittings due to orientational degeneracy of the Al-X center are summarized in Table II.

As shown in Sec. III, the ground state of the Al-X center is a twofold state and would only shift under stress. This is in contrast to the group-III acceptors in silicon, which have fourfold Γ_8 ground state. The crystal-field splitting of the ground state of the Al-X center due to its trigonal distortion could have resulted in this effect. The central-cell corrections would be much larger for the ground state which is not well described by the effective-mass theory. The excited states, on the other hand, would have much smaller central-cell corrections and could retain the fourfold symmetry. Jones *et al.*[5] have argued that the crystal-field splitting of the ground state is larger than 10 meV. Spectra taken up to 50 K showed no signs of components arising from the split-off upper ground state.

TABLE II. The eigenvalues of the stress-induced sublevels of a Γ_8 state of the Al-X center for $\mathbf{F}||\langle 111 \rangle$ and $\langle 100 \rangle$. $\delta_h=a(S_{11}+2S_{12})T$, $\Delta_{111}=(d/\sqrt{3})S_{44}T$, and $\Delta_{100}=2b(S_{11}-S_{12})T$.

Direction of $\mathbf{F}$	State	Eigenvalue
$\langle 111 \rangle$	$\Gamma_5+\Gamma_6$	$\delta_h+\delta E^{(1)}+\frac{\Delta_{111}}{2}$
	Γ_4	$\delta_h+\delta E^{(1)}-\frac{\Delta_{111}}{2}\left[1+\frac{\Delta_{111}}{\lambda}\right]$
	$\Gamma_5+\Gamma_6$	$\delta_h+\delta E^{(2),(3),(4)}+\frac{\Delta_{111}}{2}$
	Γ_4	$\delta_h+\delta E^{(2),(3),(4)}-\frac{\Delta_{111}}{2}\left[1+\frac{\Delta_{111}}{\lambda}\right]$
$\langle 100 \rangle$	Γ_6	$\delta_h+\delta E^{(1),(2),(3),(4)}+\frac{\Delta_{100}}{2}$
	Γ_7	$\delta_h+\delta E^{(1),(2),(3),(4)}-\frac{\Delta_{100}}{2}\left[1+\frac{\Delta_{100}}{\lambda}\right]$

A. Applied force along the [111] axis

We denote the stress-induced components of lines 2 and 4 as A-B, where $A=2$ and 4 and $B=1$, 2, 3, and 4. The energies of these components as a function of stress are given by

$$E_{A\text{-}1}=E_A+\delta'_h+\delta E^{(1)}-\frac{\Delta_{111}}{2}\left[1+\frac{\Delta_{111}}{\lambda}\right], \tag{3}$$

$$E_{A\text{-}2}=E_A+\delta'_h+\delta E^{(1)}+\frac{\Delta_{111}}{2}, \tag{4}$$

$$E_{A\text{-}3}=E_A+\delta'_h+\delta E^{(2),(3),(4)}-\frac{\Delta_{111}}{2}\left[1+\frac{\Delta_{111}}{\lambda}\right], \tag{5}$$

$$E_{A\text{-}4}=E_A+\delta'_h+\delta E^{(2),(3),(4)}+\frac{\Delta_{111}}{2}. \tag{6}$$

In these equations E_A are the zero-stress positions of lines 2 and 4. δ'_h is the combined hydrostatic shift of the ground and excited states. One has

$$E_{A\text{-}2}-E_{A\text{-}1}=E_{A\text{-}4}-E_{A\text{-}3}=\Delta_{111}\left[1+\frac{\Delta_{111}}{2\lambda}\right] \tag{7}$$

$$E_{A\text{-}3}-E_{A\text{-}1}=E_{A\text{-}4}-E_{A\text{-}2}=\delta E^{(2),(3),(4)}-\delta E^{(1)}. \tag{8}$$

Figure 7 shows a plot of the splittings for line 2. The solid points are the average of $E_{2\text{-}3}-E_{2\text{-}1}$ and $E_{2\text{-}4}-E_{2\text{-}2}$. The open squares are the average of the separations $E_{2\text{-}2}-E_{2\text{-}1}$ and $E_{2\text{-}4}-E_{2\text{-}3}$. The curves passing through the data are due to a least-squares fit. As predicted by Eqs. (7), (8), and (1), the fit is parabolic for the open squares and and linear for the solid points. A similar analysis has been performed for line 4 also. The values of

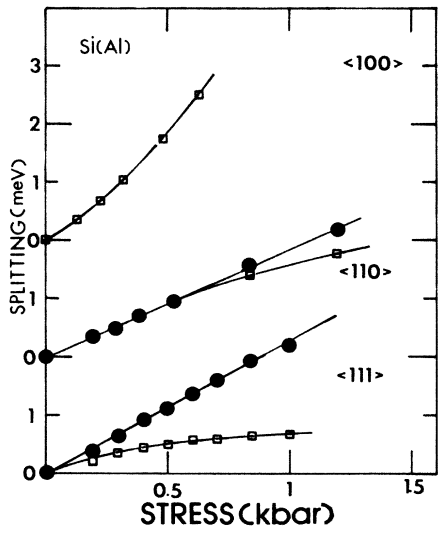

FIG. 7. Average of the energy spacing between the stress-induced components 2-3—2-1 and 2-4—2-2 as a function of stress for $\mathbf{F}\|\langle 111\rangle$ and $\langle 110\rangle$ is shown by the solid points. The average of the energy spacing 2-2—2-1 and 2-4—2-3 for $\mathbf{F}\|\langle 111\rangle$ and $\langle 110\rangle$ and 2-2—2-1 for $\mathbf{F}\|\langle 100\rangle$ is shown by the open squares. The solid curves passing through the data represent fits by the method of least squares to the equations given in the text.

χ for lines 2 and 4 for $\mathbf{F}\|\langle 111\rangle$ are 2.73 ± 0.03 and 0.72 ± 0.05 eV, respectively. The values of d (we use subscripts to denote the line) are $d_2=-1.86\pm0.04$ eV and $d_4=-3.70\pm0.11$ eV. From the nonlinear term of Eq. (7), we obtain d^2/λ for lines 2 and 4 as -2535 and -3903 eV, respectively. Using the values of d determined from the linear term, one gets the values λ for lines 2 and 4 as -1.37 and -3.51 meV. (See Table III.)

B. Applied force along the [001] axis

For $\mathbf{F}\|[001]$, $\delta E^{(1),(2),(3),(4)}=0$ and lines 2 and 4 should split, in general, into two components. The energies of these components are given by

$$E_{A\text{-}1}=E_A+\delta'_h+\frac{\Delta_{100}}{2} \tag{9}$$

and

$$E_{A\text{-}2}=E_A+\delta'_h-\frac{\Delta_{100}}{2}\left[1+\frac{\Delta_{100}}{\lambda}\right]. \tag{10}$$

Figure 7 shows a plot of the splitting

$$E_{2\text{-}2}-E_{2\text{-}1}=-\Delta_{100}\left[1+\frac{\Delta_{100}}{2\lambda}\right]$$

for line 2 by open squares. The curve passing through the data was obtained by the method of least squares. We obtain $b_2=1.24\pm0.03$ eV and $b_2^2/\lambda_2=-1331$ eV. Using b_2 obtained from the linear term of the fit, $\lambda_2=-1.16$ meV. Line 4 does not split under stress. Hence, $b_4=0$. The deformation-potential constant χ for $\langle 100\rangle$ is also zero for lines 2 and 4 since $\delta E^{(1),(2),(3),(4)}=0$.

C. Applied force along the [110] axis

For $\mathbf{F}\|[110]$, one expects four compounds each for lines 2 and 4. Following the same notation as used for [111], we have

$$E_{A\text{-}3}-E_{A\text{-}1}=E_{A\text{-}4}-E_{A\text{-}2}=\delta E^{(2),(4)}-\delta E^{(1),(3)} \tag{11}$$

and

$$E_{A\text{-}2}-E_{A\text{-}1}=E_{A\text{-}4}-E_{A\text{-}3}==(\tfrac{1}{3}\mu)^{1/2}\left[1+\frac{\nu}{\mu\lambda}\right]. \tag{12}$$

Figure 7 shows a plot of the data for line 2 and fits by the method of least squares. From Eqs. (2) and (11), we obtain χ for lines 2 and 4 for [110] as 4.56 ± 0.04 and 4.45 ± 0.10 eV, respectively.

From the definitions of μ and ν and the data for $\mathbf{F}\|\langle 100\rangle$ and $\langle 111\rangle$, one can determine Δ_{110}, which should be compared to the experimentally determined values. From the fit to the data for line 2, we get 1.92 ± 0.04 eV, which compares well with 1.67 ± 0.40 eV obtained from the data for $\langle 100\rangle$, and $\langle 111\rangle$. For line 4 the corresponding values are 2.04 ± 0.19 and 2.30 ± 0.40 eV, which are again in good agreement. The data for $\langle 110\rangle$ are hence consistent with the data for $\langle 100\rangle$, and $\langle 111\rangle$, taken in the context of Eq. (12).

TABLE III. Deformation-potential constants of Al-X center in silicon.

Direction of **F**	Line 2 ⟨111⟩	Line 2 ⟨100⟩	Line 2 ⟨110⟩	Line 4 ⟨111⟩	Line 4 ⟨100⟩	Line 4 ⟨110⟩
χ	2.73±0.03	0	4.56±0.04	0.72±0.05	0	4.45±0.10
b		1.24±0.03			0	
d	−1.86±0.04			−3.70±0.11		
λ	−1.37	−1.16		−3.51		

V. CONCLUSIONS

The piezospectroscopic study of Al-X centers in silicon has yielded values for the deformation-potential constants associated with shifts of the ⟨111⟩-oriented X centers and those of the excited states of lines 2 and 4. It is shown that the X-center complex has a trigonal rather than tetrahedral symmetry with the preferred axes along the ⟨111⟩, directions. The ground state is a twofold state (unlike a fourfold Γ_8 state). These results are consistent with those of Jones *et al.*[5] However, the nature of the complex whether it involves oxygen, boron, or carbon, cannot be conclusively stated. There is considerable speculation[5–9] on that count and it can only be resolved by a careful study of the x centers as a function of the concentration of the alleged complex-forming defects.

ACKNOWLEDGMENTS

This work was supported by the U.S. Department of Energy under Contract No. DE-AC02-84ER 45048. The stress measurements were performed at the Physics Department of Purdue University, with support from National Science Foundation Grants No. DMR-81-06144 and No. DMR-84-03325.

[1]A. K. Ramdas and S. Rodriguez, Rep. Prog. Phys. **44**, 1297 (1981).
[2]A. Onton, P. Fisher, and A. K. Ramdas, Phys. Rev. **163**, 686 (1967).
[3]R. Baron, M. H. Young, J. K. Neeland, and O. J. Marsh, Appl. Phys. Lett. **30**, 594 (1977).
[4]W. Scott, Appl. Phys. Lett. **32**, 540 (1978).
[5]C. E. Jones, D. Schafer, W. Scott, and R. J. Hager, J. Appl. Phys. **52**, 5148 (1981).
[6]M. C. Ohmer and J. E. Lang, Appl. Phys. Lett. **34**, 750 (1979).
[7]V. Swaminathan, J. E. Lang, P. M. Heminger, and S. R. Smith, Appl. Phys. Lett. **35**, 184 (1976).
[8]G. W. Ludwig and H. H. Woodbury, in *Solid State Physics*, edited by F. Seitz and D. Turnbull (Academic, New York, 1962), Vol. 13, p. 223.
[9]J. Schneider (private communication).
[10]N. R. Butler, Ph.D. thesis, Purdue University, 1974 (unpublished).
[11]V. J. Tekippe, H. R. Chandrasekhar, P. Fisher, and A. K. Ramdas, Phys. Rev. B **6**, 2348 (1972).
[12]H. R. Chandrasekhar, P. Fisher, A. K. Ramdas, and S. Rodriguez, Phys. Rev. B **8**, 3836 (1973).
[13]H. R. Chandrasekhar, A. K. Ramdas, and S. Rodriguez, Phys. Rev. B **12**, 5780 (1975).
[14]It should be pointed out that the $2p'(+)$ line of aluminum acceptors in silicon splits further into two components for $\mathbf{F}\|\langle 111\rangle$. This was attributed to a slight departure from the tetrahedral symmetry of the aluminum acceptors. The symmetry was postulated to be trigonal with the preferred axes along ⟨111⟩. (See Fig. 4 of Ref. 13.) The absence of crystal-field splitting of the ground state at zero stress, unlike in the Al-X center, suggests that the trigonal distortion is much smaller for aluminum acceptors compared to the Al-X centers.
[15]C. Herring, Bell Syst. Tech. J. **34**, 237 (1955); C. Herring and E. Vogt, Phys. Rev. **101**, 944 (1956).
[16]S. Rodriguez, P. Fisher, and F. Barra, Phys. Rev. B **5**, 2219 (1972).
[17]Effects due to the strain dependence of spin-orbit interaction lead to additional deformational-potential constants which are additive to the ones defined above. These constants are shown to be small (see Ref. 13) and are of the order of the errors in our experimental data. Hence, we shall not explicitly discuss them in our analysis.